formation potential constants. The effective mass Hamiltonian H_k for $\boldsymbol{k}\cdot\boldsymbol{p}$ perturbation is[4]

$$\begin{aligned} H_k=&A(k_x^2+k_y^2+k_z^2)-B\left[k_x^2\left(J_x^2-\frac{1}{3}J^2\right)\right.\\ &\left.+k_y^2\left(J_y^2-\frac{1}{3}J^2\right)+k_z^2\left(J_z^2-\frac{1}{3}J^2\right)\right]\\ &-\frac{2}{3}N[\{k_xk_y\}\{J_xJ_y\}+\{k_xk_z\}\{J_xJ_z\}\\ &+\{k_yk_z\}\{J_yJ_z\}]\ ; \end{aligned} \tag{3.2}$$

Under high stress, one is able to treat H_k in the Hamiltonian $H=H_e+H_k$ as the perturbation to H_e. It has been calculated to second order by Hasegawa.[11] The values of A, B, N, D_u and $D_{u'}$ can be so determined as the experimental and theoretical effective masses agree most nicely with each other over the angle θ between the stress and magnetic field directions for the transition ($n=0\rightarrow1$) and over the stress for those ($n=0\rightarrow1$ and $n=1\rightarrow2$). Use is made of the relation

$$\left(\frac{1}{m^*}\right)^2=\frac{\cos^2\theta}{m_\perp{}^2}+\frac{\sin^2\theta}{m_\perp m_{/\!/}}\ ; \tag{3.3}$$

whence we treat two cases of stress direction.

Case I $\chi//\langle111\rangle$

In eq. (3.3) we put

$$m_\perp=\frac{1}{A-\frac{N}{6}(1-4x)}\quad\text{and}\quad m_{/\!/}=\frac{1}{A+\frac{N}{3}(1-4x)}$$

for the transition ($n=0\rightarrow1$, $M_j=-\frac{1}{2}$);

where $x=\dfrac{\varepsilon'}{\lambda}$, $\varepsilon'=\dfrac{D_{u'}\chi}{3c_{44}}$ and λ is the spin-orbit coupling constant. For a particular orientation $H//\langle111\rangle$, we find the expression of effective mass for the transition $n\rightarrow n+1$:

$$\frac{m^*}{m_0}=\frac{1}{A-\frac{N}{6}(1-4x)-\dfrac{\left(B^2+\frac{2N^2}{9}\right)n}{\dfrac{4\varepsilon'}{\dfrac{\hbar eH}{m_0c}}}}\ ,$$

for $M_j=-\dfrac{1}{2}$,

and

$$\frac{m^*}{m_0}=\frac{1}{A-\frac{N}{6}(1-4x)-\dfrac{\frac{1}{2}\left(B^2+\frac{2N^2}{9}\right)+\frac{1}{4}\left(B^2+\frac{2N^2}{9}\right)n}{\dfrac{\varepsilon'}{\dfrac{\hbar eH}{m_0c}}}}\ , \tag{3.4}$$

for $M_j=+\dfrac{1}{2}$.

Case II $\chi//\langle100\rangle$

We put

$$m_\perp=\frac{1}{A-\frac{B}{2}(1-4x)}\quad\text{and}\quad m_{/\!/}=\frac{1}{A+B(1-4x)}\ ,$$

in eq. (3.3);

where $x=\dfrac{\varepsilon}{\lambda}$ and $\varepsilon=\dfrac{2D_u\chi}{3(c_{11}-c_{12})}$.

For $H//\langle100\rangle$, we have

$$\frac{m^*}{m_0}=\frac{1}{A-\frac{1B}{2}(1-4x)-\dfrac{\frac{3}{8}\left\{\left(B\pm\frac{1}{3}N\right)^2+\left(B^2+\frac{N^2}{9}\right)n\right\}}{\dfrac{\varepsilon}{\dfrac{\hbar eH}{m_0c}}}}\ , \tag{3.5}$$

according as $M_j=\pm\dfrac{1}{2}$.

Both in Figs. 4 and 5, the theoretical variations of the effective masses are given by the solid lines. We may note the peak ($n=2\to3$, $M_j=-\frac{1}{2}$) coincides with that of ($n=0\to1$, $M_j=+\frac{1}{2}$) in the case χ, $H//\langle111\rangle$ in eq. (3.4). Agreement between theory and experiment is not so good for large quantum numbers and in the low stress region, for the second order perturbation becomes questionable on one hand while the resolution of the lines becomes worse. With a moderate stress and at temperature below 4.2°K, population of carriers on the levels $M_j=\pm\frac{3}{2}$ is small and can be safely neglected in the present analysis.

In the treatment given so far, the Zeeman shift of the energy has been neglected, because it is smaller than the strain shift by an order of magnitude for the strain of 1.0×10^{-3}. An extra term associated with this Zeeman shift, however, should be taken into account in the low strain region as well as for large quantum numbers. We may calculate the energy levels by a different approach; *i.e.*, diagonalization of the total Hamiltonian $H=H_e+H_k+H_{\text{Zeeman}}$, under the assumption $B=N/3$.[19] The value for g-factor (2κ) can be obtained from Figs. 5(a) and 5(b) through fitting the diagonalization curves (dashed) with the experimental data. In the diagonalization approach, the M_j classification employed so far is replaced by the notations $a^{\pm}$ and $b^{\pm}$ in accordance with Gurgenishivili.[24]

§ 4. Linewidth of the Quantum Line

In the case that carriers are scattered by the thermal lattice vibrations, Bardeen and Shockley[15] made a theoretical calculation for mobilities of electrons and holes in nonpolar crystals. The scattering probability was calculated for isotropic phonons ($c_{44}=\frac{1}{2}(c_{11}-c_{12})$) by the deformation potential method, in which the carriers in a strained lattice feel a local energy disturbance δE proportional to the strain components e_{ij}; *i.e.*,

$$\delta E=\sum_{ij}\Xi_{ij}e_{ij}\,. \tag{4.1}$$

Here Ξ_{ij} is the deformation potential constant for electron. Herring and Vogt extended the above method to the case of many valley semiconductors with an approximate anisotropic dispersion relation for phonons.[16] The relaxation time can be simplified in the ellipsoidal constant energy surface. In order to calculate the relaxation time of holes in germanium under uniaxial compression, it is necessary to construct an interaction term analogous to eq. (4.1). When the uniaxial stress is applied along the $\langle111\rangle$ direction, the corresponding interaction Hamiltonian is given by eq. (3.1). It is a good approximation to solve eq. (3.1) through the second order perturbation in the high stress limit. The reason why we can use the Herring-Vogt method is that the originally warped energy surfaces for holes, under the application of uniaxial stress, become nearly ellipsoidal around the axis of stress, thus simulating themselves to those for electrons. The final result is given in terms of the usual second rank tensor:

$$\mathbf{D}=\begin{pmatrix} D_d^V & -\frac{1}{3}D_{u'} & -\frac{1}{3}D_{u'} \\ -\frac{1}{3}D_{u'} & D_d^V & -\frac{1}{3}D_{u'} \\ -\frac{1}{3}D_{u'} & -\frac{1}{3}D_{u'} & D_d^V \end{pmatrix}. \tag{4.2}$$

It is worth noting that eq. (4.2) does not contain the parameter D_u, that is, it is described only by two parameters D_d^V and $D_{u'}$. The corresponding expression for the relaxation time of hole becomes

$$\frac{1}{\tau_\perp}=(3\pi Ck_BT\varepsilon^{1/2}/Vc_l)(\xi_\perp D_d^{V^2}+\eta_\perp D_d^V D_{u'}+\zeta_\perp D_{u'}^2); \tag{4.3}$$

where

$$C=(m_\perp^2 m_{//})^{1/2}\,V/2^{3/2}\pi^2\hbar^4\,,$$

$$c_l=c_{12}+2c_{44}+\frac{3}{5}c^*$$

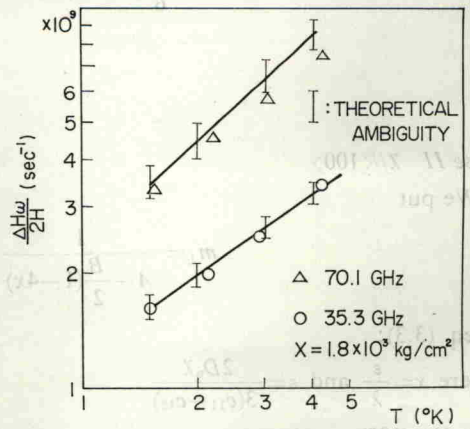

Fig. 6. Temperature dependence of linewidth of the hole cyclotron transition ($n=0\to1$, $M_j=-\frac{1}{2}$) under the conditions shown. The theoretical curves are fitted to the experimental values at 1.5°K. Theoretical ambiguity arises from the difficulty of determining the positions to measure the half-width; namely, the resonance lines may oscillate in the high magnetic field region, owing to the terms $\sum_n(E-n\eta)^{-1/2}$ in eq. (4.4).